

ReFace: Improving Clothes-Changing Re-Identification With Face Features

Daniel Arkushin*¹ Bar Cohen*² Shmeul Peleg¹ Ohad Fried²

¹The Hebrew University of Jerusalem ²Reichman University

<http://www.vision.huji.ac.il/reface/>

{daniel.arkushin, peleg}@mail.huji.ac.il bar.cohen01@post.runi.ac.il ofried@runi.ac.il

Abstract

*Person re-identification (ReID) has been an active research field for many years. Despite that, models addressing this problem tend to perform poorly when the task is to re-identify the same people over a prolonged time, due to appearance changes such as different clothes and hairstyles. In this work, we introduce a new method that takes full advantage of the ability of existing ReID models to extract appearance-related features and combines it with a face feature extraction model to achieve new state-of-the-art results, both on image-based and video-based benchmarks. Moreover, we show how our method could be used for an application in which multiple people of interest, under clothes-changing settings, should be re-identified given an unseen video and a limited amount of labeled data. We claim that current ReID benchmarks do not represent such real-world scenarios, and publish a new dataset, **42Street**, based on a theater play as an example of such an application. We show that our proposed method outperforms existing models also on this dataset while using only pre-trained modules and without any further training.*

1. Introduction

Person re-identification (ReID) aims to match the same people appearing at different times and locations. As explained in Section 2.1, in a typical ReID setting, the predicted label of each query sample is defined based on a given gallery set. Most commonly used ReID benchmarks [19, 30, 35, 45], capture people within a single day, where clothes are rarely changed [12]. These benchmarks were used by models that rely on clothes and not necessarily on unique person characteristics [11, 14, 36]. To enable ReID research under clothes-changing settings, benchmarks including clothes changes, such as LTCC [29], PRCC [41] and CCVID [13] have been released. To solve this problem, several models try to extract clothes-independent, global features [1, 12, 29, 40, 41].

*These authors contributed equally

In spite of the efforts invested in solving the clothes-changing problem, ReID models still perform better in the same-clothes setting [12]. Current ReID models do not use explicit face features [9] — although, when available, face features distinguish between people with much higher accuracy, across different times and environments. Therefore, we suggest a method that relies on both clothes features and face features to automatically enrich a given labeled gallery in a weakly supervised manner (Section 3.1). Our model combines face feature extraction and ReID modules (Section 3.2) and achieves new state-of-the-art results. We note that every module of our method could be replaced by new ReID or face models having better capabilities.

In existing clothes-changing ReID benchmarks, data samples are clear crops of a single person to be re-identified. Moreover, these benchmarks address the closed-set setting only, and therefore, do not represent real-world scenarios which include occlusions, crowded scenes, and open-set settings (see Section 2.1 for more details). We show how our method, when using a tracking module, can address such complex scenarios and release a new dataset, **42Street** (Section 4.2) as an example for a real-world application. We show that without any further training our method achieves strong results on this dataset while outperforming the existing ReID models.

Our contribution in this work is twofold:

1. We suggest a method that combines ReID and face modules, and enriches a given gallery using face features, to achieve new state-of-the-art results on existing clothes-changing ReID benchmarks.
2. We publish a new dataset, **42Street**, as an example for an application of person ReID on a complex real-world scenario, and show that our method achieves strong results on it while outperforming existing models.

2. Background and Related Work

2.1. Person Re-Identification

The inference process of person ReID can be seen as an instance retrieval problem. Given labeled data samples and unlabeled query samples, the goal is to predict the correct label for every query sample. In a standard ReID pipeline, first, a gallery is created by applying a feature-extraction model (the ReID model) on the labeled samples to represent them using feature vectors. Next, given an unseen query sample, the distances between its feature vector and the gallery feature vectors are computed. Finally, the predicted label of the query sample is defined as the label of the gallery feature vector which is closest to the query. A typical ReID dataset provides train and test sets that do not share common identities.

To address the ReID challenge, in addition to using RGB images, several models suggest using different input modalities such as depth images [37], text descriptions [18], infrared images [38], and more.

Image-based and Video-based ReID In image-based ReID datasets, every data sample is a single-person crop. Over the years, multiple image-based models have been developed [14, 23, 24, 36], and they achieve impressive results on image-based benchmarks. In video-based ReID datasets, every data sample is a sequence of crops and the ReID model produces a single feature vector to represent the entire sequence by using the spatial-temporal information in the sequence [10, 12, 15, 27].

Clothes-changing ReID In this setting, a person in the query set might wear different clothes than in the gallery set. Some models try to extract clothes-independent features by modeling body shape and gait using skeletons [29], silhouettes [1] and contour sketches [40]. Another model, CAL [12], proposes a Clothes-based Adversarial Loss to mine clothes-independent features, and uses the video input to extract spatio-temporal patterns. Training these models requires ground-truth clothes annotations.

Open-Set and Closed-Set A closed-set setting assumes that every identity in the query set has at least one corresponding sample in the gallery set. In an open-set setting, this might not be the case, as some identities in the query are not present in the gallery. Open-set ReID is usually formulated as a person verification problem in which a model is required to discriminate whether two person images belong to the same identity [34, 46]. Models that address this problem [21, 22, 39], typically learn to discriminate between a given query and gallery according to their similarity [17].

3. Method

In order to address the clothes-changing ReID problem, our method enriches the labeled gallery (Section 3.1) and combines standard ReID approaches together with face feature extraction (Section 3.2). Both elements work in conjunction and define our method. Our method can be applied to image-based, video-based, and raw-video input.

3.1. Creating an Enriched Gallery

The objective of most ReID models is to produce a feature extraction function that generates a feature vector for each data sample. Given two different data samples of the same person, the feature extraction function is expected to generate feature vectors with a lower cosine distance compared to two samples from different persons. The richer the gallery is with samples that are similar to the query set, the more likely it is to find a correct gallery match. Hence, we propose an algorithm to enrich a given labeled gallery using face features, when available, from the unlabeled query.

Building an enriched gallery is done using the following weakly supervised algorithm and summarized in Fig. 1. Given labeled and unlabeled samples:

1. For every labeled data sample in which a face was detected, we extract a face feature vector and label it using the label of the original sample, to create a face gallery.
2. For every unlabeled sample in which a face was detected and verified (Section 3.1.1), we predict a label by computing its face feature vector and comparing it to the labeled face gallery from step 1.
3. (optional) Under the open-set setting, we label out-of-gallery queries as "Unknown" (Section 3.3).
4. We create an enriched gallery by extracting ReID feature vectors from the originally labeled data and the predicted samples from step 2.

We note that the above process assumes that the query set is given beforehand, however, this process could also be made online by adding one query sample at a time.

3.1.1 Matching Face to Pose Estimation

A person crop is a part of an image cropped according to the posture of a specific person. Often, in person crops from crowded scenes, multiple people appear in the background of a person's crop. In such cases, a face detected in an image might belong to a person in the background and not to the main person according to whom the crop was created. Therefore, it is necessary to verify whether the detected face belongs to the main person in the crop. To do this, we use a separate pose estimation of the main person in the crop and verify that the keypoints of the eyes and nose, as given

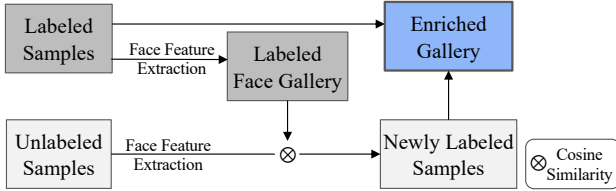


Figure 1. **The Gallery Enrichment Process.** For every labeled sample in which a face was detected, a face feature vector is extracted to create a labeled face gallery. Then, for every unlabeled sample in which a face was detected, a label is predicted by computing cosine similarities between its face feature vector and the labeled face gallery. Finally, an enriched gallery is created by extracting ReID features from both the original labeled samples and the newly labeled samples.

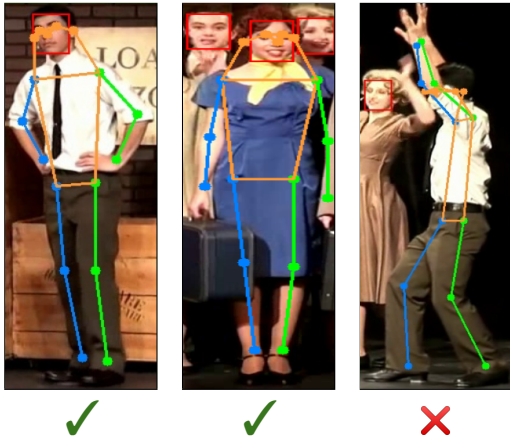


Figure 2. **Matching Face Detection and Pose Estimation.** *Left:* A single detected face that matches the main person. *Middle:* Multiple detected faces, the main person’s pose matches one of the detected faces. *Right:* A single detected face that does not match the pose estimation of the main person.

by the pose estimator, are within the bounding box given by the face detector. Examples are shown in Fig. 2.

3.2. Combining ReID and Face Modules

In our method we propose to use a face feature extraction module and a ReID module to compute face and ReID score vectors respectively. These score vectors represent the confidence of each module that the given track belongs to each of the possible identities. Our method combines these two score vectors into a final score vector which is used to label the identity of the person in a given data sample. Next, we describe in detail our method for the video-based setting, where every data sample is a person track. The prediction process for the image-based setting is treated as a special case of the video-based setting, in which a data sample, i.e. a single image, is a track of length 1.

Predicting an Identity of a Track Given labeled data of a set of identities I , we first build an enriched gallery, $G_{enriched}$, as described in Section 3.1, and a labeled face gallery denoted G_{face} , by extracting face feature vectors from the labeled data. Then, given a person track, we apply the face feature extraction and the ReID modules on it to create a score vector of size $|I|$, representing the confidence of our model that the given track belongs to each identity in I . This process is illustrated in Fig. 3 and detailed next.

Face and ReID Score Vectors Given a person track with N consecutive image crops of the same person, denote $v_{ReID} \in \mathbb{R}^{|I|}$ to be a vector representing the ReID score for each identity, initialized with zeros.

For every image q in the track, we compute the feature vector representing this image using the ReID module. Then, for each identity $i \in I$ the confidence that image q belongs to identity i is defined as the maximum cosine-similarity between the feature vector of q and the feature vectors of all gallery samples of identity i in $G_{enriched}$. The final score for identity i , i.e. $v_{ReID}[i]$, is the mean confidence for identity i for all the images in the track.

Denote $v_{face} \in \mathbb{R}^{|I|}$ to be a vector representing the face score for each identity, initialized with zeros. To compute v_{face} we follow the same procedure as above while changing the input images and gallery. In this case, the input images for the procedure are M detected face images from the original person track. Those are created by applying a face-detector on every image in the original track, and verifying that the pose matches the main person in the image (Section 3.1.1). The gallery used for similarity comparison is the labeled face gallery G_{face} .

Combining Score Vectors To compute the final score vector $v_{pred} \in \mathbb{R}^{|I|}$, similarly to Wan et al. [33], we take a linear combination of the output of the two score vectors with a hyper-parameter α . The resulting score vector is:

$$v_{pred} = \alpha \cdot v_{ReID} + (1 - \alpha) \cdot v_{face} \quad (1)$$

The final label prediction for the entire track is given by taking the identity with the highest score in v_{pred} .

3.3. Addressing the Open-set Challenge

In the open-set setting, we approach the task of labeling an out-of-gallery query sample by utilizing the gallery enrichment process (Section 3.1). During this process we label a given query sample as “Unknown” and add it to the enriched gallery if it fulfills the following criteria:

1. A face was detected with confidence above a certain threshold, and verified (Section 3.1.1).

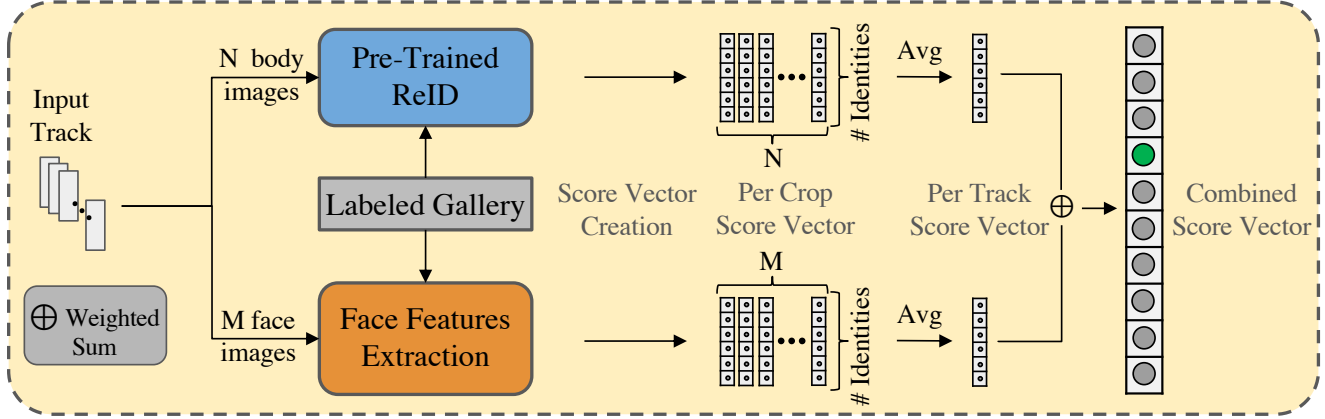


Figure 3. **Track Identity Prediction Overview.** Given an input track, using all track images, the ReID and face modules produce a track score vector representing the confidence of every module that the track belongs to each of the possible identities. Then, these score vectors are combined into a final score vector and the track is labeled according to the identity with the highest score (green circle).

2. The cosine similarity between the feature vector of the detected face and the labeled face gallery feature vectors is below a certain threshold.
3. The difference between the rank-1 and rank-2 predictions in the face score vector is below a certain threshold.

3.4. Raw-Video ReID: A Real-World Application

In order to apply our method to a given raw-video, we use a tracking module without applying any changes to it. The tracker module detects and tracks people across multiple frames and outputs a sequence of per person image crops (tracks). For each track, we predict an identity as described in Section 3.2. Finally, the tracks and their predictions are displayed on the input video to create an annotated output video. This process is illustrated in Fig. 4.

4. Evaluation

In this section, we list the models we compare our results against and provide details for the evaluation of existing clothes-changing ReID benchmarks (Section 4.1). Then, we describe the *42Street* dataset curation (Section 4.2) and detail the protocol to evaluate the performance of various models on the clothes-changing ReID scenarios in it.

4.1. Evaluation on Existing Benchmarks

We evaluate the performance of our model and compare it with CAL [12], CTL [36], and InsightFace [5–8]. CAL is a clothes-changing ReID model, CTL is a model that focuses on the same-clothes setting, and InsightFace is a face analysis project. All models are evaluated on four widely used clothes-changing ReID benchmarks: three image-based benchmarks, LTCC [29], PRCC [41], and LAST [31], and one video-based benchmark, CCVID [13]. For consistency with the results reported by CAL, the current SoTA

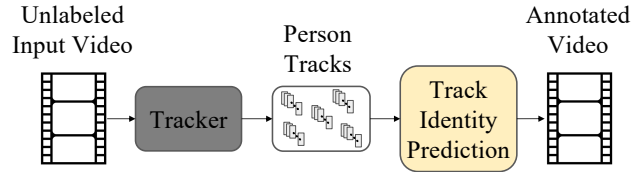


Figure 4. **Raw-Video Annotation overview.** Given an unlabeled video, person tracks are generated using a tracking module. Next, the identity of each track is predicted in the Track Identity Prediction process (Fig. 3). Finally, all tracks and their predicted identities, are displayed on the input video to create an annotated video.

model on these benchmarks, Top-1 accuracy and mAP are used as evaluation metrics and three kinds of test settings are defined as follows:

- *General*: both clothes-changing and same-clothes ground truth samples are used to calculate accuracy.
- *Clothes-Changing (CC)*: only clothes-changing ground truth samples are used to calculate accuracy.
- *Same-Clothes (SC)*: only same-clothes ground truth samples are used to calculate accuracy.

4.2. The 42Street Dataset

As described in Section 1, current clothes-changing ReID benchmarks do not represent complex real-world scenarios with open-set settings. For this reason, we create and publish the *42Street* dataset, as an evaluation dataset, i.e. we do not provide training data with a different set of identities, compared to the test set.

The dataset is created using a public recording of the 42Street theatre play [26]. The play is ~ 1.5 hours long and was split into 5 equally long parts of ~ 20 minutes each, with various clothes changes between the different parts.

From *Part 1* we label samples that are used by our method and other models we compare against. Parts 2–3 and 4–5 are used for validation and test, respectively, and from them, we randomly extract 5 validation videos and 10 test videos, each 17 seconds long. We define a set of people-of-interest I , which consists of 13 people that appear in all parts of the play in various clothes, and define a single class, “Unknown”, for all people that are not part of set I .

In Appendix D, we describe a semi-supervised process for generating labeled samples quickly. As this process requires relatively low effort, our method can be easily applied to new unseen data.

Annotating Evaluation Videos To annotate an evaluation video with ground truth labels, a tracker, ByteTrack [43], is applied to automatically extract tracks of detected people, followed by a manual annotation of every track. These ground-truth labels, as well as person bounding boxes, track ids, video names, and more are saved in a designated database published alongside the dataset. In Appendix E, we provide more details about the database and how it can be used for further research and to reproduce our results.

Evaluation on the 42Street Dataset Given the labeled samples created from *part 1* of the play, we evaluate the performance of our method on the evaluation videos (Section 4.2) of the *42Street* dataset and compare it with the same models as described in Section 4.1. In addition, we also compare the results of the video-based version of CAL for which we provide labeled video samples. As the *42Street* dataset is an evaluation dataset only, all models are evaluated without any fine-tuning.

Evaluation Metrics The *42Street* dataset represents a real-world scenario in which, given a raw-video, a model should produce a single prediction for each person crop detected in the video. Therefore, we measure a model’s performance using classification metrics: *Per-Image* and *Per-Track* accuracy. We note that these accuracies are equivalent to the top-1 metric, typically used in ReID works.

- *Per-Image Accuracy*: the number of correctly identified person crops in a video, divided by the total number of person crops in the video, across all evaluation videos.
- *Per-Track Accuracy*: the number of correctly classified tracks, i.e. whether the model’s single prediction on the entire track is correct, divided by the total number of tracks in the video, across all evaluation videos.

We note that the image-based models we evaluate generate a per-image prediction, and do not provide a single

prediction for an entire track. In order to address this limitation, while calculating their *Per-Track* accuracy, we set a single prediction for the entire track based on the most confidently predicted identity, across all the track images, similarly to Section 3.2. Furthermore, as this work does not focus on improving tracking capabilities, while calculating this metric any track with less than 10 frames is ignored, as those are likely to be tracking mistakes.

Open-Set and Closed-Set ReID Settings ReID models we compare our results against assume that the input datasets are of a closed-set setting. Hence, in order to correctly evaluate against these models we compare the results in both the open-set and closed-set settings. The latter is done by ignoring out-of-gallery queries during evaluation.

5. Experiments

5.1. Setting Hyper-Parameters

A typical face-detection model produces a confidence score that a face exists in a given image. Additionally, cosine distances between the face feature vector of the input image and a face gallery are calculated. These distances can be used as the confidence that the given input image belongs to a certain identity. To achieve the best results, we set thresholds for both confidence scores. Given a dataset, we apply our gallery enrichment method (Section 3.1) on the training set to find the best combination of these two thresholds. Ideally, we would like to find the optimal combination that achieves the highest prediction accuracy based on face features, whilst maintaining a high detection accuracy per person. Meaning, we would like the model to predict at least one image of each identity in order to create an enriched gallery with examples of all identities. However, there exists a trade-off between the per-identity detection accuracy and the prediction accuracy: for a higher detection threshold, the number of unique predicted identities decreases. At the same time, since the detected faces are of better quality, the prediction accuracy increases. Vice versa, a lower detection threshold, leads to a larger number of predicted identities, while achieving lower prediction accuracy. Fig. 6 demonstrates this trade-off for the PRCC benchmark.

5.2. Implementation Details

For our face module, we use *InsightFace* [5–8] for face detection, alignment, and feature extraction. For the ReID module, we examine both CTL [36], pre-trained on DukeMTMC [30] and CAL [12]. The hyper-parameter α used for combining the face score vector and the ReID score vector in Eq. (1) is set to 0.75, giving more weight to the ReID module.

The detection and similarity thresholds used by our face

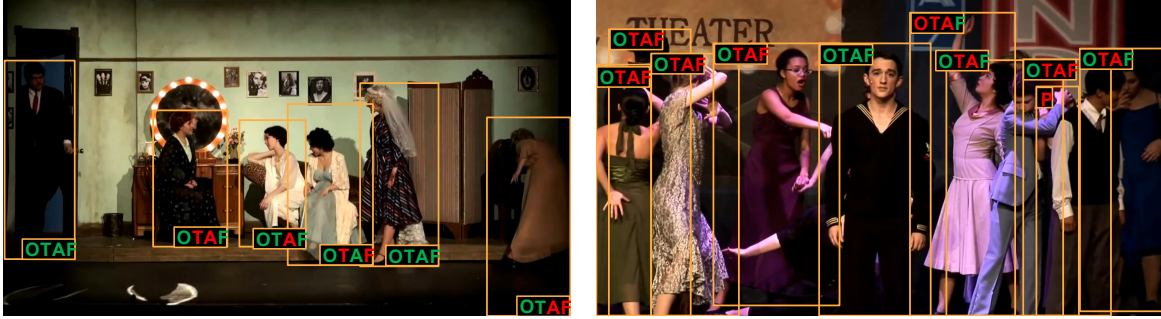


Figure 5. **Performance Visualization on the 42Street Dataset.** Results visualization of the different compared models under the closed-set setting (left) and open-set setting (right). For each bounding box, the abbreviation 'OTAF' refers to the different models — O (Ours), T (CTL), A (CAL), F (InsightFace). The green and red colors correspond to a correct and incorrect prediction of each model on the bounding-box. In the open-set frame (right), all people other than the one in the center are out-of-gallery and should be labeled as "Unknown".

Method	CCVID		LTCC				PRCC				LAST	
	General		General		CC		SC		CC		General	
	top-1	mAP	top-1	mAP	top-1	mAP	top-1	mAP	top-1	mAP	top-1	mAP
<i>CTL</i>	71.8	64.8	36.7	11.1	11.7	4.8	78.6	68.8	24.0	21.0	20.1	3.2
<i>CAL</i>	82.9	81.3	74.4	41.2	40.1	19.0	100	99.8	55.7	56.3	73.7	28.8
<i>InsightFace</i>	95.3	N/A	27.4	9.2	24.5	8.3	95.6	70.0	77.9	54.7	57.8	31.1
<i>Ours</i>	89.2	N/A	75.5	41.2	48.2	19.8	99.7	95.6	83.7	66.7	78.0	38.1

Table 1. **Models comparison on existing clothes-changing benchmarks.** *Ours* refers to our method using CAL as the ReID module, CAL was fine-tuned on each benchmark and CTL was pre-trained on DukeMTMC. *General* considers all gallery samples for evaluation, *SC* considers only same-clothes gallery samples, and *CC* considers only clothes-changing gallery samples. Notice that our model outperforms other models on most benchmarks, and especially in the clothes-changing setting. We note that although the face model achieves the best results on CCVID, the results on other benchmarks suggest that it is insufficient by itself.

module (Section 5.1) are determined according to the training set for the existing benchmarks, and the validation set for the *42Street* dataset. In Appendix F, we detail all the thresholds used for the different datasets.

For *42Street*, the entire raw videos of test-set parts are used as query input for the gallery enrichment process. In Appendix C, we analyze the impact of using more raw-data for the gallery enrichment process. To apply our method on the real-world application described in Section 3.4, we use ByteTrack [43] as our tracking module as well as the MCV [3] and MMTRACK [4] frameworks. To deal with some of the tracking limitations, as the original play includes many scene cuts, i.e. abrupt changes of the camera angle or zoom, we apply a scene cut detection algorithm, and split tracks accordingly if necessary.

5.3. Results

Next, we present the results of the compared models on existing clothes-changing ReID benchmarks as well as on the *42Street* dataset and show the significant improvement that can be achieved by using our method. In Appendix B,

we provide an ablation study of the various components in our method and their significance.

5.3.1 Existing Benchmarks Results

Table 1 compares the results of our method versus the evaluated models on the existing clothes-changing ReID benchmarks. From the table, we notice that our method significantly outperforms the other evaluated models on all benchmarks, except for the SC setting on PRCC where it achieves comparable results to the current SoTA model. In addition, we note that although the face model achieved superior results compared to other models on CCVID, the results on other benchmarks suggest that it is not sufficient by itself. This is due to the nature of the CCVID benchmark, which was curated from a gait-recognition dataset (FVG [44]), recording people as they walk toward the camera with clearly visible faces.

We note that as explained in Section 3.2, given an input track, our model produces a score vector representing the confidence that the track belongs to each of the possible identities. Therefore, as our model does not rank all gallery

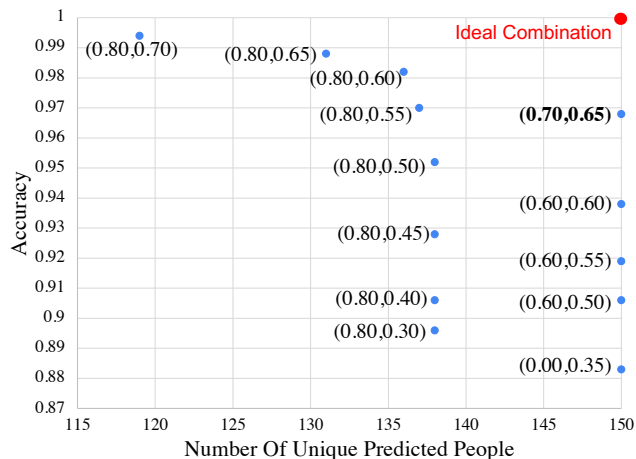


Figure 6. **Prediction Accuracy vs. Number of Unique People.** Example of the thresholds trade-off on the PRCC benchmark. Each data tuple represents the values of the detection threshold (left) and similarity threshold (right). We look for the combination that achieves the highest prediction accuracy while predicting the highest number of unique people (bold).

Method	PRCC \rightarrow LTCC				LTCC \rightarrow PRCC			
	General		CC		SC		CC	
	top-1	mAP	top-1	mAP	top-1	mAP	top-1	mAP
<i>CAL</i>	21.9	6.1	7.4	3.3	99.5	99.7	39.3	36.5
<i>CTL</i>	36.7	11.1	11.7	4.8	78.6	68.8	24.0	21.0
<i>Our-CAL</i>	27.8	6.9	16.6	3.9	99.7	100	81.5	53.0
<i>Our-CTL</i>	40.8	11.8	21.4	5.5	91.7	58.3	78.3	32.9

Table 2. **Cross-Dataset Generalization without Fine-Tuning.** Results comparison using a pre-trained ReID model, without fine-tuning on the evaluated dataset. $X \rightarrow Y$ means that *CAL* was pre-trained on dataset *X* and evaluated on dataset *Y*. *CTL* was pre-trained on DukeMTMC. In *Ours(X)*, *X* refers to the ReID model our method used.

tracks, we cannot calculate mAP for the video-based benchmark CCVID.

5.3.2 Cross-Dataset Results

Next, we analyze the generalization ability of different models. In this experiment, we evaluate the performance of the compared models on PRCC and LTCC without fine-tuning on the evaluated benchmark. We compare the performance of *CAL*, pre-trained on LTCC when evaluated on PRCC and vice versa, *CTL*, pre-trained on DukeMTMC, and our model, both with *CAL* and *CTL* as the ReID module. Table 2 summarizes the results of this experiment and shows that our model has better generalization abilities to unseen data than existing ReID models.

5.3.3 42Street Dataset Results

Table 3 compares the results of our method versus the evaluated models on the *42Street* dataset.

Under the closed-set setting, similar to the results of the cross-dataset experiment (Section 5.3.2), it is clear from the table that both *CTL* and *CAL* models have limited generalization ability on the *42Street* dataset as well. Furthermore, the face-recognition model itself achieves only mediocre results. This is due to the fact that in the *42Street* dataset the face detector detected faces only in 74% of the total person crops, some of which are not of sufficient quality to be recognized correctly. However, our method, whilst not requiring any further training, achieves strong results and significantly outperforms the other models.

Under the open-set setting, all other evaluated models achieve poor results, as they are not designed to address this setting. However, by using simple adaptations as described in Section 3.3, our method is able to handle the open-set challenge and achieve solid results. Fig. 5 visualizes the performance of the various models under both settings.

As image-based models are not capable of generating a single prediction for a track, per-track accuracy cannot be directly calculated for them. In Table 5, we provide an extended table with the results of such models when adapted to generate predictions over tracks.

We note that the accuracy results on the *42Street* dataset concern only the detected person crops. The person detector of ByteTrack [43] which we used, achieved an IDF1 score of 80.5 for the MOT17 [25] challenge. As such, results for all evaluated models could potentially be discounted by a 19.5% margin to bridge the possible gap of misidentified person crops. On the other hand, additional tracker limitations, as described in Section 5.4, may affect the ability of our method to correctly classify a track. These limitations do not impact the image-based models we compare against, as their input is a single crop and not a track.

5.4. Limitations

Our method heavily relies on the assumption that every clothes-set of each identity has at least one high quality face-image within the given labeled samples and query sets. For datasets that do not hold this assumption due to limited number of detected faces or low quality of the detected faces, our method would only show slight improvement over other models, as only a limited amount of query samples will be added to the original gallery in the gallery enrichment process. That said, we believe our assumption holds for many real-world scenarios and as such can introduce significant improvement compared to existing models on such scenarios.

To apply our method to real-world applications and annotate a raw-video we use a tracking module to extract person tracks. Using a tracker introduces several limitations:

Method	Closed-Set		Open-Set	
	Per Image	Per Track	Per Image	Per Track
<i>CTL</i>	0.31	N/A	0.20	N/A
<i>CAL-Image</i>	0.20	N/A	0.13	N/A
<i>CAL-Video</i>	0.21	0.16	0.26	0.17
<i>InsightFace</i>	0.55	N/A	0.36	N/A
<i>Ours-CTL</i>	0.92	0.81	0.79	0.65

Table 3. **Models comparison on the 42Street dataset.** All models are evaluated under both closed-set and open-set settings. The models are pre-trained on other datasets and are not fine-tuned on this dataset: *CTL* on DukeMTMC, *CAL-Image* on LTCC, *CAL-Video* on CCVID. *Ours(X)* refers to using our model with X as the ReID module. Note, as *CTL*, *CAL-Image* and *InsightFace* are image-based models, per track accuracy is not applicable for them.

- Identity Switch - often, when dealing with person occlusions in crowded scenes, the tracker begins with tracking one person and mistakenly switches to a different person. In this case, track-based predictions which provide a single prediction for the entire track, incorrectly label the 'switched' part of the track.
- Missed Detected Persons - people that were not identified by the tracker's person detector module.
- Incorrectly Detected Persons - occurs when the person detector of the tracker "detects" a non-existing person.

Currently, our method uses a tracking module without applying any changes to it, and does not deal with these potential tracking mistakes.

6. Ethical Considerations

The release of new person ReID and tracking datasets often raises privacy concerns as individuals that appear in the dataset are not always asked for their consent. To comply with the regulations on data collection and usage, such as European General Data Protection Regulation (GDPR) and California Consumer Privacy Act (CCPA), some papers suggest data anonymization by removing identifying information and blurring faces [28, 32]. Since our work depends on the existence of faces in the dataset, blurring is not an option, however, we address this concern by using publicly available videos only. Furthermore, while our method utilizes face features to improve ReID performance it is only used for image retrieval and distance measurement and does not require any further identity matching or recognition. Another ethical consideration is the usage of ReID and tracking systems. While these systems have many positive applications for public safety, improving city planning, etc., they could also be used maliciously, to spy on and sup-

press people. Our method and published dataset should only be used for academic purposes.

7. Discussion & Future Work

In this work, we show a novel approach to address the clothes-changing ReID challenge by creating an enriched gallery from the given labeled and unlabeled samples, based on face features. By combining the enriched gallery with face feature extraction and ReID modules, our proposed method achieves state-of-the-art results on clothes-changing ReID benchmarks and on the real-world clothes-changing dataset we publish, *42Street*. Furthermore, our method shows that with minimal labeling efforts, solid results can be achieved on raw-videos, without any further training. This is in contrast to current models that lack the ability to generalize to unseen data.

Future work ideas to improve our method include:

- Use the fact that two people that appear in the same frame, cannot receive the same label.
- Use complete tracks instead of a single crop in the gallery enrichment process. This could make the gallery both richer and more accurate.
- Support real-time gallery enrichment, by adding extracted face and ReID features to the galleries in inference time.

A. Extended Results

In Table 4 we compare the results of additional clothes-changing ReID models. Since not all papers have released their code, the reported results are taken from the original papers. From the table we learn that our method outperforms these models as well.

Table 5 shows the results of different models on the *42Street* dataset. In addition to the image-based versions of these models presented in the paper, the track-based version is shown in order to support evaluation according to the *Per Track* metric. This version is created in a similar way to the track inference process (Section 3.2).

In Table 6 we evaluate the performance under two additional settings compared to the results shown in the paper: *Clothes-Changing (CC)* for the CCVID benchmark, and *General* for the PRCC benchmark.

The *General* setting for the PRCC benchmark is calculated using a weighted average of the *Same-Clothes* and *Different-Clothes* settings. Even though it is not provided by previous works, we include this setting as it is important to understand the overall performance of the model. From the table we can see that under this setting as well, our method significantly outperforms the other models.

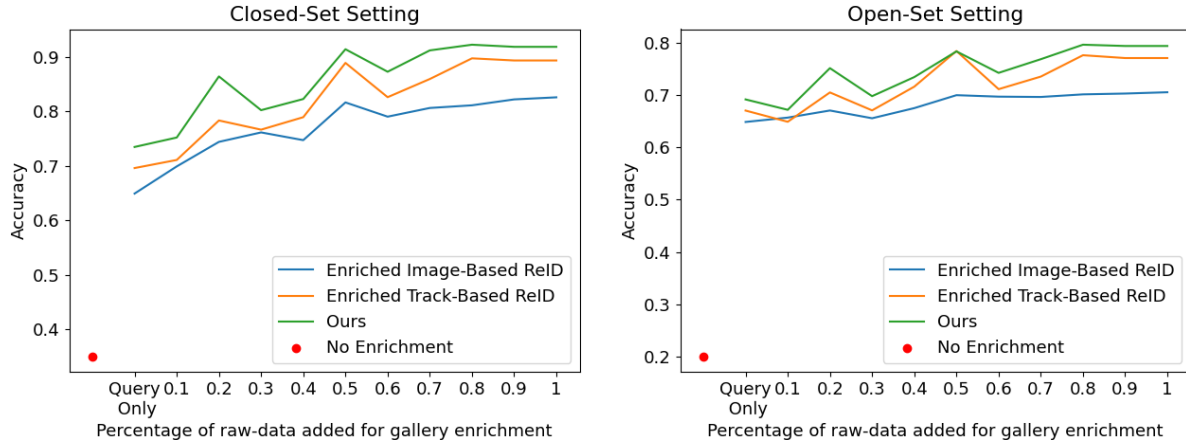


Figure 7. Accuracy as a function of the percentage of additional raw data used for gallery enrichment in the *42Street* dataset. This figure shows the impact of gallery enrichment with a ReID module(CTL), while using additional raw-data on both closed-set (left) and open-set (right) settings. The X-axis shows the percentage of raw-data that is used in the gallery enrichment process. The red point represents the results of the image-based ReID module, without using any enrichment. *Query Only* refers to using only the data in the evaluation videos for the gallery enrichment process. Each step represents the percentage of additional data from the raw-video of the test part that was used in the gallery enrichment process. The results suggest that enriching the gallery using the *Query Only* data, significantly improves the same ReID module compared to no enrichment. Moreover, the total accuracy of all compared modules increases when using more raw-data.

Method	LTCC (CC)		PRCC (CC)	
	top-1	mAP	top-1	mAP
<i>CAL</i> [12]	40.1	19.0	55.7	56.3
<i>CACC</i> [20]	40.3	18.4	57.4	–
<i>LCVN</i> [42]	–	–	64.4	62.6
<i>3DSL</i> [2]	31.2	14.8	51.3	–
<i>FSAM</i> [16]	38.5	16.2	54.5	–
<i>Our</i>	48.2	19.8	83.7	66.7

Table 4. Additional models comparison on LTCC and PRCC. We evaluate the performance under the clothes-changing setting only (CC) as this is the only setting included in the original papers.

B. Ablation Study

In this section we evaluate the impact of each component of our method on the overall performance of our method, both on the existing benchmarks and the *42Street* dataset. From Table 7 and Table 8 we conclude the following:

- The *Gallery Enrichment Process* introduces a significant improvement compared to using only a ReID module, without enrichment. In Appendix C, we further discuss the influence of additional raw data on the performance of our method.
- Combining ReID and face modules (even without gallery enrichment), significantly improves the results of current ReID models.

Method	Closed-Set		Open-Set	
	Per Image	Per Track	Per Image	Per Track
<i>CTL</i>	0.31	N/A	0.20	N/A
<i>CTL (Track)</i>	0.35	0.27	0.21	0.15
<i>CAL-Image</i>	0.20	N/A	0.13	N/A
<i>CAL-Image (Track)</i>	0.22	0.22	0.12	0.11
<i>CAL-Video</i>	0.21	0.16	0.26	0.17
<i>InsightFace</i>	0.55	N/A	0.36	N/A
<i>InsightFace (Track)</i>	0.69	0.62	0.45	0.36
<i>Ours-CTL</i>	0.92	0.81	0.79	0.65

Table 5. Extended models comparison on the *42Street* dataset. Image-based models predict an identity per-image, and therefore are not evaluated on the Per-Track accuracy metric. To address this, a (Track-Based) prediction is calculated using a track score vector, generating a single prediction for the entire track. All evaluated models are pre-trained on other datasets: CTL on DukeMTMC; CAL-Image on LTCC; CAL-Video on CCVID. *Ours* refers to using our model with CTL as the ReID module.

- The face module by itself achieves superior results compared to the original ReID module. Although this shows the strength of face features and their importance for ReID tasks, it is not a sufficient model as not all images include a clearly visible face.
- Examining the *Per Image Acc* in Table 8 shows that the track-based version of the different modules improves the results compared to their image-based versions.

Method	CCVID				PRCC					
	General		CC		General		SC		CC	
	top-1	mAP	top-1	mAP	top-1	mAP	top-1	mAP	top-1	mAP
<i>CTL</i>	71.8	64.8	69.3	61.2	52.5	46.0	78.6	68.8	24.0	21.0
<i>CAL</i>	82.9	81.3	81.9	79.6	78.8	79.0	100	99.8	55.7	56.3
<i>InsightFace</i>	95.3	N/A	73.5	N/A	87.1	62.7	95.6	70.0	77.9	54.7
<i>Ours-CAL</i>	89.2	N/A	90.5	N/A	92.1	81.8	99.7	95.6	83.7	66.7

Table 6. **Extended models comparison on existing clothes-changing benchmarks.** In this table, in addition to the results shown in the paper for CCVID and PRCC, we present the clothes-changing setting for CCVID and the general setting for PRCC. *Ours* refers to our method using CAL as the ReID module, CAL was fine-tuned on each benchmark and CTL was pre-trained on DukeMTMC. *General* considers all gallery samples for evaluation, *SC* considers only same-clothes gallery samples, and *CC* considers only clothes-changing gallery samples. Additionally to the results shown in the paper, we note that under the CC setting in CCVID, our model also outperforms Insightface, as the number of clothes-changing gallery samples is significantly lower, which leads to the lower performance of this model. For PRCC, the general setting is computed as the weighted sum between the SC and CC settings, i.e. computed according to the relative sizes of the CC and SC query samples, and was added to provide a comparison of the overall performance of each model.

- The open-set setting leads to weaker results of all components, as it introduces a more difficult challenge of verification, i.e. labeling an out-of-gallery query sample as “Unknown”.
- **Our method, combining ReID and face modules with an enriched gallery achieves the best results on the evaluated datasets.**

C. Using Raw-Data For Gallery Enrichment

As explained in the *42Street* dataset creation (Section 4.2), the test data of this dataset consists of two parts from the play, each around 20 minutes long. Out of these parts, we extract short videos, 17-seconds each, for evaluation. In this section, in addition to enriching the gallery with the query data (from the evaluation videos), we analyze the impact of using more raw-data (from the test part) for the gallery enrichment process. We start by using only the evaluation videos for gallery enrichment, and gradually add more randomly sampled raw data from the test parts. Fig. 7 shows the accuracy of the compared models as a function of the amount of raw-data used for the gallery enrichment process. Notice that the initial gallery enrichment with query data only, already introduces a significant improvement compared to not using enrichment at all, and that the accuracy increases as we add more raw-data. This is true for the Image-based ReID model, Track-based ReID model and our method, on both the closed and open set settings, with the best results achieved by our method. Even though raw-data is not available in the standard ReID task, we argue that such data is common in real-world scenarios like the application we presented, and show how it can be used to boost the performance of our method.

D. Creation of Labeled Galleries

In this section, we explain in detail how to create labeled face and full-body crop data samples, in a generic, semi-supervised process. We provide the details for the *42Street* dataset as an example, but this process can be applied on every raw-data video.

This process is illustrated in Fig. 8 and works as follows:

1. Given the entire video of the first part (*Part I*) of the *42Street* play, which is allocated for gallery creation, apply a person detector on every frame in the video.
2. For each detected person-crop, use face detection and feature extraction modules to extract face features.
3. Apply K-means clustering over all face feature vectors with a high number of clusters compared to $|I|$ ($K \gg |I|$), where I is the set of people of interest.
4. Manually iterate over each cluster, remove images that are not of the main person in the cluster and label the cluster as one of the identities in I .
5. For each newly labeled face image, automatically label the matching full-body crop image with the same label.
6. Save both labeled full-body crops and face images to generate labelled galleries.

We note that the manual traversal and labeling of clusters took approximately 2 hours, to curate ~ 500 images per identity, with a total of $\sim 8K$ labeled images.

Method	General		Same-Clothes		Changing-Clothes	
	top-1	mAP	top-1	mAP	top-1	mAP
<i>ReID Module</i>	78.8	79.0	100	99.8	55.7	56.3
+ <i>Enriched Gallery</i>	91.3	77.3	99.7	93.1	82.2	60.0
<i>Face Module</i>	87.1	62.7	95.6	70.0	77.9	54.7
<i>ReID + Face Modules</i>	91.2	73.2	99.8	83.3	81.9	62.2
<i>Ours-CAL</i>	92.1	81.8	99.7	95.6	83.7	66.7

Table 7. **Ablation study of our method on the PRCC benchmark.** *ReID+Face Modules* is the combination of both face and ReID modules without gallery enrichment. *Ours* is the complete proposed model that uses both face and ReID modules, and an enriched gallery. The ReID module used is CAL.

Method	Closed-Set		Open-Set	
	Per Image Acc	Per Track Acc	Per Image Acc	Per Track Acc
<i>ReID Module (Image-based)</i>	0.31	N/A	0.20	N/A
+ <i>Enriched Gallery</i>	0.83	N/A	0.71	N/A
<i>ReID Module (Track-based)</i>	0.31	0.27	0.21	0.15
+ <i>Enriched Gallery</i>	0.88	0.76	0.77	0.61
<i>Face Module (Image-based)</i>	0.55	N/A	0.36	N/A
<i>Face Module (Track-based)</i>	0.69	0.62	0.45	0.36
<i>ReID + Face Modules</i>	0.81	0.67	0.50	0.38
<i>Ours-CTL</i>	0.92	0.81	0.79	0.65

Table 8. **Ablation study of our method on the 42Street dataset.** *Image/Track-based* refers to whether the labeling decision of the model is done per a single image or on the entire track, respectively. *ReID + Face Modules* is the combination of both face and ReID modules without gallery enrichment. *Ours* is the complete proposed model that uses both face and ReID modules, and an enriched gallery. The ReID module used is CTL. Note, that *Per Track Acc* is not applicable for image-based models.

E. The 42Street Database

We save each labeled crop from the *42Street* dataset in a designated database, which includes spatial and temporal information for each crop. Every entry in the database includes the following information:

- *label*.
- *im_name*: unique entry.
- *frame_num*: the number of the frame in the video from which the crop was taken.
- *x1,y1,x2,y2*: top-left and bottom-right coordinates of the bounding box.
- *conf*: the confidence of the person detector that a person exists in the crop.
- *vid_name*: the name of the video from which the crop was taken
- *track_id*: the track number given by the tracker.
- *crop_id*: the number of the crop within the track.
- *invalid*: a boolean that is set to true for crops that do not present a clear person.

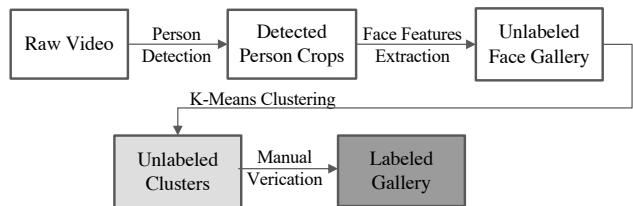


Figure 8. **Process of Labeled Gallery Creation** The above process describes how a raw video is proceeded into labeled full-body and face galleries. For the *42Street* dataset, manual traversal and labeling of clusters took approximately 2 hours, to curate ~ 500 images per identity, with a total $\sim 8K$ labeled images.

F. Threshold Details

In Table 9 we detail the detection and similarity thresholds used by our method for the existing benchmarks. These thresholds are determined according to the training set for the existing benchmarks, and the validation set for the *42Street* dataset. Moreover, for the *42Street* dataset, we used the evaluation data to extract the following thresholds:

- *Detection Threshold*: for the gallery enrichment process we used a threshold of 0.8 and during inference we used 0.7. The reason we use a higher threshold

Threshold	Detection	Similarity
CCVID	0.5	0.75
LTCC	0.8	0.5
PRCC	0.7	0.65
LaST	0.7	0.45

Table 9. **Threshold values for existing benchmarks.** The different detection and similarity thresholds used for the gallery enrichment process in each of the existing benchmarks.

for the gallery enrichment process is that we are interested in creating a highly accurate gallery. On the other hand, during inference we want to use more images with faces, and we are more tolerate for mistakes.

- *Similarity Threshold:* during the gallery enrichment process we use a threshold of 0.4 for the cosine similarity between an unlabeled sample and the labeled gallery. That is, if the maximal cosine similarity between the feature vector of the unlabeled sample and the labeled gallery is below this threshold, this sample will not be added to the enriched gallery.
- *Rank Difference:* in addition to detecting only clearly visible faces with a high similarity to the labeled gallery, we want to use only samples for which the face model was confident about their identity. We measure this confidence as the difference between the similarity score of the top-1 and top-2 predictions of the model. In the *42Street* dataset, if the difference is below 0.1, we do not add the sample to the enriched gallery.

Under the open-set setting, to label people which are not in the people-of-interest set as “Unknown”, we set another threshold. This threshold asserts that a person will be labeled as “Unknown” if the similarity to all people-of-interest is below 0.3. Meaning that whilst having high detection confidence, the model is not confident of the identity.

References

- [1] Hanqing Chao, Yiwei He, Junping Zhang, and Jianfeng Feng. Gaitset: Regarding gait as a set for cross-view gait recognition. *CoRR*, abs/1811.06186, 2018. 1, 2
- [2] Jiaying Chen, Xinyang Jiang, Fudong Wang, Jun Zhang, Feng Zheng, Xing Sun, and Wei-Shi Zheng. Learning 3d shape feature for texture-insensitive person re-identification. In *2021 IEEE/CVF Conference on Computer Vision and Pattern Recognition (CVPR)*, pages 8142–8151, 2021. 9
- [3] MMCV Contributors. MMCV: OpenMMLab computer vision foundation. <https://github.com/open-mmlab/mmcv>, 2018. 6
- [4] MMTracking Contributors. MMTracking: OpenMMLab video perception toolbox and benchmark. <https://github.com/open-mmlab/mtracking>, 2020. 6
- [5] Jiankang Deng, Jia Guo, Tongliang Liu, Mingming Gong, and Stefanos Zafeiriou. Sub-center arcface: Boosting face recognition by large-scale noisy web faces. In *Proceedings of the IEEE Conference on European Conference on Computer Vision*, 2020. 4, 5
- [6] Jiankang Deng, Jia Guo, Xue Niannan, and Stefanos Zafeiriou. Arcface: Additive angular margin loss for deep face recognition. In *CVPR*, 2019. 4, 5
- [7] Jiankang Deng, Jia Guo, Evangelos Ververas, Irene Kotsia, and Stefanos Zafeiriou. Retinaface: Single-shot multi-level face localisation in the wild. In *CVPR*, 2020. 4, 5
- [8] Jiankang Deng, Anastasios Roussos, Grigorios Chrysos, Evangelos Ververas, Irene Kotsia, Jie Shen, and Stefanos Zafeiriou. The menpo benchmark for multi-pose 2d and 3d facial landmark localisation and tracking. *IJCV*, 2018. 4, 5
- [9] Julia Dietlmeier, Joseph Antony, Kevin McGuinness, and Noel E. O’Connor. How important are faces for person re-identification? *CoRR*, abs/2010.06307, 2020. 1
- [10] Chanho Eom, Geon Lee, Junghyup Lee, and Bumsub Ham. Video-based person re-identification with spatial and temporal memory networks, 2021. 2
- [11] Dengpan Fu, Dongdong Chen, Jianmin Bao, Hao Yang, Lu Yuan, Lei Zhang, Houqiang Li, and Dong Chen. Unsupervised pre-training for person re-identification. *Proceedings of the IEEE conference on computer vision and pattern recognition*, 2021. 1
- [12] Xinqian Gu, Hong Chang, Bingpeng Ma, Shutao Bai, Shiguang Shan, and Xilin Chen. Clothes-changing person re-identification with rgb modality only. In *CVPR*, 2022. 1, 2, 4, 5, 9
- [13] Xinqian Gu, Hong Chang, Bingpeng Ma, Shutao Bai, Shiguang Shan, and Xilin Chen. Clothes-changing person re-identification with rgb modality only. In *CVPR*, 2022. 1, 4
- [14] Lingxiao He, Xingyu Liao, Wu Liu, Xinchen Liu, Peng Cheng, and Tao Mei. Fastreid: A pytorch toolbox for general instance re-identification, 2020. 1, 2
- [15] Tianyu He, Xin Jin, Xu Shen, Jianqiang Huang, Zhibo Chen, and Xian-Sheng Hua. Dense interaction learning for video-based person re-identification, 2021. 2
- [16] Peixian Hong, Tao Wu, Ancong Wu, Xintong Han, and Wei-Shi Zheng. Fine-grained shape-appearance mutual learning for cloth-changing person re-identification. In *2021 IEEE/CVF Conference on Computer Vision and Pattern Recognition (CVPR)*, pages 10508–10517, 2021. 9
- [17] Qingming Leng, Mang Ye, and Qi Tian. A survey of open-world person re-identification. *IEEE Transactions on Circuits and Systems for Video Technology*, 30(4):1092–1108, 2020. 2
- [18] Shuang Li, Tong Xiao, Hongsheng Li, Bolei Zhou, Dayu Yue, and Xiaogang Wang. Person search with natural language description. *CoRR*, abs/1702.05729, 2017. 2
- [19] Wei Li, Rui Zhao, Tong Xiao, and Xiaogang Wang. Deepreid: Deep filter pairing neural network for person re-identification. *2014 IEEE Conference on Computer Vision and Pattern Recognition*, pages 152–159, 2014. 1
- [20] Xulin Li, Bin Liu, Yan Lu, Qi Chu, and Nenghai Yu. Cloth-aware center cluster loss for cloth-changing person re-identification. In Shiqi Yu, Zhaoxiang Zhang, Pong C. Yuen,

- Junwei Han, Tieniu Tan, Yike Guo, Jianhuang Lai, and Jian-guo Zhang, editors, *Pattern Recognition and Computer Vision*, pages 527–539, Cham, 2022. Springer International Publishing. 9
- [21] Xiang Li, Ancong Wu, and Wei-Shi Zheng. Adversarial open-world person re-identification, 2018. 2
- [22] Giuseppe Lisanti, Niki Martinel, Alberto Del Bimbo, and Gian Luca Foresti. Group re-identification via unsupervised transfer of sparse features encoding. In *2017 IEEE International Conference on Computer Vision (ICCV)*, pages 2468–2477, 2017. 2
- [23] Hao Luo, Wei Jiang, Youzhi Gu, Fuxu Liu, Xingyu Liao, Shenqi Lai, and Jianyang Gu. A strong baseline and batch normalization neck for deep person re-identification. *CoRR*, abs/1906.08332, 2019. 2
- [24] Niki Martinel, Gian Luca Foresti, and Christian Micheloni. Aggregating deep pyramidal representations for person re-identification. In *2019 IEEE/CVF Conference on Computer Vision and Pattern Recognition Workshops (CVPRW)*, pages 1544–1554, 2019. 2
- [25] A. Milan, L. Leal-Taixé, I. Reid, S. Roth, and K. Schindler. MOT16: A benchmark for multi-object tracking. *arXiv:1603.00831 [cs]*, Mar. 2016. arXiv: 1603.00831. 7
- [26] SOTA music. 42 street - the complete musical, 2013. 4
- [27] Athira Nambiar, Alexandre Bernardino, and Jacinto C. Nascimento. Gait-based person re-identification: A survey. *ACM Comput. Surv.*, 52(2), apr 2019. 2
- [28] E.M. Newton, L. Sweeney, and B. Malin. Preserving privacy by de-identifying face images. *IEEE Transactions on Knowledge and Data Engineering*, 17(2):232–243, 2005. 8
- [29] Xuelin Qian, Wenxuan Wang, Li Zhang, Fangrui Zhu, Yanwei Fu, Tao Xiang, Yu-Gang Jiang, and Xiangyang Xue. Long-term cloth-changing person re-identification. *arXiv preprint arXiv:2005.12633*, 2020. 1, 2, 4
- [30] Ergys Ristani, Francesco Solera, Roger S. Zou, R. Cucchiara, and Carlo Tomasi. Performance measures and a data set for multi-target, multi-camera tracking. In *ECCV Workshops*, 2016. 1, 5
- [31] Xiujun Shu, Xiao Wang, Xianghao Zang, Shiliang Zhang, Yuanqi Chen, Ge Li, and Qi Tian. Large-scale spatio-temporal person re-identification: Algorithms and benchmark, 2021. 4
- [32] Latanya Sweeney. K-anonymity: A model for protecting privacy. *Int. J. Uncertain. Fuzziness Knowl.-Based Syst.*, 10(5):557–570, oct 2002. 8
- [33] Fangbin Wan, Yang Wu, Xuelin Qian, and Yanwei Fu. When person re-identification meets changing clothes. *CoRR*, abs/2003.04070, 2020. 3
- [34] Hanxiao Wang, Xiatian Zhu, Tao Xiang, and Shaogang Gong. Towards unsupervised open-set person re-identification. In *2016 IEEE International Conference on Image Processing (ICIP)*, pages 769–773, 2016. 2
- [35] Longhui Wei, Shiliang Zhang, Wen Gao, and Qi Tian. Person transfer GAN to bridge domain gap for person re-identification. *CoRR*, abs/1711.08565, 2017. 1
- [36] Mikolaj Wiecek, Barbara Rychalska, and Jacek Dabrowski. On the unreasonable effectiveness of centroids in image retrieval, 2021. 1, 2, 4, 5
- [37] Ancong Wu, Wei-Shi Zheng, and Jianhuang Lai. Robust depth-based person re-identification. *CoRR*, abs/1703.09474, 2017. 2
- [38] Ancong Wu, Wei-Shi Zheng, Hong-Xing Yu, Shaogang Gong, and Jianhuang Lai. Rgb-infrared cross-modality person re-identification. In *2017 IEEE International Conference on Computer Vision (ICCV)*, pages 5390–5399, 2017. 2
- [39] Hao Xiao, Weiyao Lin, Bin Sheng, Ke Lu, Junchi Yan, Jingdong Wang, Errui Ding, Yihao Zhang, and Hongkai Xiong. Group re-identification: Leveraging and integrating multi-grain information. In *2018 ACM Multimedia Conference on Multimedia Conference*, pages 192–200. ACM, 2018. 2
- [40] Qize Yang, Ancong Wu, and Wei-Shi Zheng. Person re-identification by contour sketch under moderate clothing change. *CoRR*, abs/2002.02295, 2020. 1, 2
- [41] Qize Yang, Ancong Wu, and Wei-Shi Zheng. Person re-identification by contour sketch under moderate clothing change. *IEEE Transactions on Pattern Analysis and Machine Intelligence (DOI 10.1109/TPAMI.2019.2960509)*, 2020. 1, 4
- [42] Renjie Zhang, Yu Fang, Huaxin Song, Fangbin Wan, Yanwei Fu, Hirokazu Kato, and Yang Wu. Specialized re-ranking: A novel retrieval-verification framework for cloth changing person re-identification. *Pattern Recognition*, 134:109070, 2023. 9
- [43] Yifu Zhang, Peize Sun, Yi Jiang, Dongdong Yu, Fucheng Weng, Zehuan Yuan, Ping Luo, Wenyu Liu, and Xinggang Wang. Bytrack: Multi-object tracking by associating every detection box, 2021. 5, 6, 7
- [44] Ziyuan Zhang, Luan Tran, Xi Yin, Yousef Atoum, Xiaoming Liu, Jian Wan, and Nanxin Wang. Gait recognition via disentangled representation learning. *CoRR*, abs/1904.04925, 2019. 6
- [45] Liang Zheng, Liyue Shen, Lu Tian, Shengjin Wang, Jingdong Wang, and Qi Tian. Scalable person re-identification: A benchmark. In *Computer Vision, IEEE International Conference on*, 2015. 1
- [46] Xiatian Zhu, Botong Wu, Dongcheng Huang, and Wei-Shi Zheng. Fast open-world person re-identification. *IEEE Transactions on Image Processing*, 27(5):2286–2300, 2018. 2